

# Mass and Heat Transfer Enhancement during 3D Vibrating Drying of a Clay Porous Brick

Nidhal Ben Khedher\*

*College of Engineering, Mechanical Engineering Department, Hail University, Hail City, Saudi Arabia, City  
Laboratoire d'Études des Systèmes Thermiques et Énergétiques, Ecole Nationale d'Ingénieurs de Monastir,  
Monastir 5019 Tunisie  
Email: [nidhal.ben.khedher@gmail.com](mailto:nidhal.ben.khedher@gmail.com)*

## Abstract

A three dimensional coupled heat and moisture transfer model for vibrating convective drying process of unsaturated porous medium was established. The aim of this paper is to study the effect of vibration on the drying of whole brick. A Three-dimensional unstructured Control Volume Finite Element Method (CVFEM) is developed. In order to simulate 3-D complex geometries, as application here the drying of whole brick, we developed Fortran modules to build the polygonal CVFEM mesh based on 3-D unstructured meshes generated by the free mesh generator Gmsh. The temperature, the liquid saturation and pressure distributions for whole brick were presented and analyzed for both cases namely with and without vibration. The results obtained state that the drying process is highly enhanced by vibration and the drying time is reduced by 20%.

**Keywords:** 3D vibrating drying; CVFEM; Gmsh; unsaturated porous media.

## 1. Introduction

Technology of vibrating drying has been widely used in industry in several developed countries, and it has gained more and more attention. Since, the vibration has been found to enhance heat and mass transfer mechanisms. However, A review of literature shows that only few research papers were conducted to investigate this technique of drying. Beck and his colleagues investigate the influence of airborne ultrasound conditions on the drying [1]. Moreover, a fundamental study of the drying intensification by vibration was established by Colin and his colleagues [2].

---

\* Corresponding author.

Also, the vibration effect on convection excitation in fluid and porous layers has been studied by Kolchanova and Kolchanov [3]. The effect of high-frequency and small-amplitude vibrations on the excitation of convection in fluids and fluid-saturated porous media was widely studied [4-8].

Application of vibrational techniques for physical processing of granular materials in feeding, conveying, cooling, drying, agglomeration and milling, were reviewed by [9]. Reference [10] studied food product drying using vibro-fluidization technique. It was found that vibration intensity should be lower than 3.3. The suitable values of vibration intensity and amplitude were 1.5–2.0 and 5–10 mm, respectively.

More recently, Ramzi and his colleagues has developed a 3-D numerical model to study the vibration effects on drying process [11]. The motivation of this study is that the vibration is a new technology for the amelioration of drying process which deserves more attention.

In this context, the aim of the present paper is to offer a numerical study that is able to evaluate the external vibration effect on drying process through a comparison between two cases; classical convective drying and triangular vibrating drying. For this reason, a 3-D numerical model is employed to describe the coupled heat and mass transfer phenomena during vibrating drying of unsaturated porous plate.

The control volume finite element method (CVFEM) is employed. A review of the literature unveils little evidence of where CVFEM has been used to simulate numerically the physics associated with heat and mass transfer in porous materials [12-13]. References [14-15] have used the finite element method to study similar problems. However, they found that the CVFEM was superior for reasons concerning efficiency, conservation, and robustness across a wide range of varying drying conditions of isotropic and anisotropic porous material.

The 3-D drying kinetics (average water content, temperature and pressure profiles) will be exhibited for the vibration during high temperature drying of whole brick. Several simulation numerical results studying the effect of vibration on drying process, are presented and analyzed.

## **2. Mathematical model**

The proposed problem is an industrial problem treating the vibrating drying of whole brick which is an industrial problem.

The system considered in this work is a whole brick (porous medium) which is composed of:

- An inert and rigid solid phase (brick matrix).
- A liquid phase (pure water).
- A gaseous phase which contains both air and water vapor.

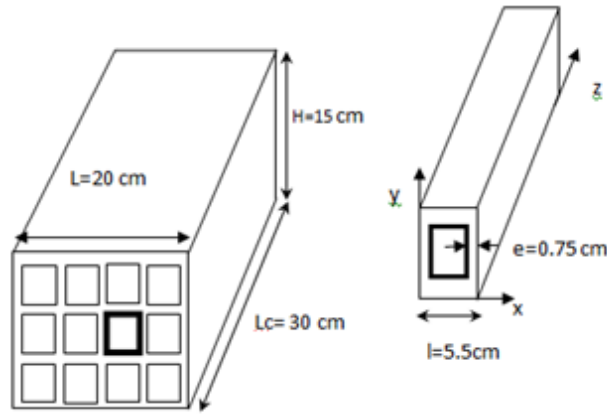


**Figure 1:** Whole clay brick dimensions.

### 2.1. Governing equations

The proposed model is based on a numerical problem treating an external vibrations of hot air on heat and mass transfer during the drying of unsaturated porous medium process.

The numerical model is a comparison of heat and mass transfer during drying process for three configurations of drying (hot air velocity):

- Without vibration

$$V_a = 10 \text{ m/s} \quad (1)$$

- With triangular vibration

$$V_a = a \times t + b \text{ (m/s)} \quad (2)$$

With:

$$\begin{cases} a = \frac{3 \times A_v}{T_v}, b = 0 & ; 0 \leq t \leq \frac{T_v}{3} \\ a = \frac{-6 \times A_v}{T_v}, b = 3 \times A_v; & \frac{T_v}{3} \leq t \leq \frac{2 \times T_v}{3} \\ a = \frac{3 \times A_v}{T_v}, b = -3 \times A_v; & \frac{2 \times T_v}{3} \leq t \leq T_v \end{cases}$$

With  $A_v$  is the maximum amplitude of vibrating velocity,  $t$  is the time,  $T_v$  and  $f_v$  are respectively the period and the frequency of vibrating velocity and  $a$  is the acceleration.

The periodic evolutions of hot air velocity for the two configurations of vibrating drying are presented in Fig. 2.

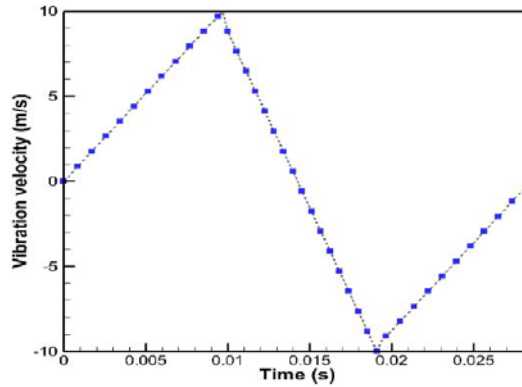


**Figure 2:** Evolution of hot air velocity during a period for triangular vibration

Based on Whitaker theory, a mathematical model governing heat and mass transfer is established for the unsaturated porous media. In order to obtain a closed set of governing macroscopic equations, the following assumptions are made:

- The porous layer is homogenous and isotropic.
- The solid, liquid and gas phases are in local thermodynamic equilibrium.
- The compression-work and viscous dissipation are negligible.
- The gas-phase is ideal in the thermodynamic sense.
- The dispersion and tortuosity terms are interpreted as diffusion term.
- The radiative heat transfer is negligible.

Considering these assumptions, macroscopic equations governing heat and mass transfer in the porous medium are:

- Generalized Darcy's Law:

The average velocities of the liquid phase ( $\bar{V}_l$ ) and the gas phase ( $\bar{V}_g$ ) are obtained using Darcy's Law which is generalized by using the concept of relative permeability defined as the ratio between the effective permeability and the intrinsic permeability.

For the liquid phase:

$$\bar{V}_l = -\frac{KK_l}{\mu_l} \left[ \nabla \left( \bar{P}_g^g - P_c \right) - \bar{\rho}_l^l g \right] \tag{1}$$

With  $P_c = \bar{P}_g^g - \bar{P}_l^l$  : the capillary pressure.

For the gas phase (without taking into consideration the gravitational effect):

$$\overline{V}_g = -\frac{KK_g}{\mu_g} \nabla \overline{P}_g^g \tag{2}$$

▪ Mass conservation equations:

• Liquid phase:

Assuming that liquid density is constant, the mass conservation equation of the liquid phase is:

$$\frac{\partial \varepsilon_l}{\partial t} + \nabla(\overline{V}_l) = -\frac{\dot{m}}{\rho_l} \tag{3}$$

Where  $\dot{m}$  is the mass rate of evaporation and  $\varepsilon_l$  is the volume fraction of liquid phase.

• Gas phase:

For this phase the average density is not constant. In this case, the mass conservation equation of the gas phase is given by:

$$\frac{d\overline{\rho}_g}{dt} + \nabla(\overline{\rho}_g \overline{V}_g) = \dot{m}_g \tag{4}$$

Where  $\overline{\rho}_g$  is the intrinsic average density of the gas phase. This phase is considered as an ideal mixture of perfect gases.

• Vapor phase:

$$\frac{d\overline{\rho}_v}{dt} + \nabla(\overline{\rho}_v \overline{V}_v) = \dot{m}_v \tag{5}$$

$$\overline{\rho}_v \overline{V}_v = \overline{\rho}_v \overline{V}_g - \overline{\rho}_g D_{eff} \nabla \left( \frac{\overline{\rho}_v}{\overline{\rho}_g} \right) \tag{6}$$

$D_{eff}$  represents the coefficient of the effective diffusion of the vapor in the porous medium. This coefficient takes into account the resistance to the diffusion due to tortuosity and the effects of constriction.

▪ Energy conservation equation:

$$\frac{\partial}{\partial t}(\overline{\rho C_p T}) + \text{div} \left[ \left( \overline{\rho_l C_{pl} v_l} + \sum_{k=a,v} \overline{\rho_k^g C_{pk} v_k} \right) \overline{T} \right] = \nabla \cdot (\lambda_{\text{eff}} \cdot \nabla \overline{T}) - \Delta H_{\text{vap}} \cdot \mathbf{i}_v \quad (7)$$

$\Delta H_{\text{vap}}$  is the latent heat of vaporization at temperature T(K).

$\lambda_{\text{eff}}$  and  $\overline{\rho C_p}$  are respectively the effective thermal conductivity and the constant pressure heat capacity of the porous medium and  $\overline{\rho C_p}$  is given by:

$$\overline{\rho C_p} = \overline{\rho_s} C_{ps} + \overline{\rho_l} C_{pl} + \overline{\rho_a} C_{pa} + \overline{\rho_v} C_{pv} \quad (8)$$

Where  $\overline{\rho_s} C_{ps}$ ,  $\overline{\rho_l} C_{pl}$ ,  $\overline{\rho_v} C_{pv}$  and  $\overline{\rho_a} C_{pa}$  are respectively the mass heat capacities of the brick solid matrix, liquid, vapor and air.

- Thermodynamic relations:

The partial pressure of the vapor is equal to its equilibrium pressure:  $P_v = P_{\text{veq}}(T, S)$ .

Where S is the liquid saturation defined by:

$$S = \frac{\varepsilon_l}{\varepsilon} \quad (9)$$

The gaseous phase is assumed to be an ideal mixture of perfect gases:

$$\overline{P_i} = \frac{\overline{\rho_i}}{M_i} R \overline{T} \quad ; i=a,v \quad (10)$$

$$\overline{P_g} = \overline{P_a} + \overline{P_v}, \quad \overline{\rho_g} = \overline{\rho_a} + \overline{\rho_v}$$

Vapor Pressure:

$$\frac{P_v}{P_{vs}} = \exp \left( - \frac{2 \cdot \sigma \cdot M_v}{r \cdot \rho_l \cdot R \cdot T} \right) \quad (11)$$

## 2.2 Boundary and initial conditions

Initially, the temperature, the gas pressure and liquid saturation are uniform in the brick. Thermal energy

brought by air convection is necessary for water evaporation and to the heat conduction in porous medium. This energy is function of temperature and heat transfer coefficient.

On the exchanging faces (holes and sides (right, left and top)), we can write:

$$\left[ \lambda_{eff} \frac{\partial \langle T \rangle}{\partial X_i} + \Delta H_{vap} \rho_l \langle V_l \rangle n_i \right] = h_t (\langle T \rangle - T_\infty) \tag{12}$$

The mass flow corresponding to evaporation and to the evacuation of water is function of the vapor density difference and mass transfer coefficient:

$$\left[ \rho_l \langle V_l \rangle + \langle \rho_v \rangle^g \langle V_v \rangle \right] n_i = h_m (C_{vs} - C_{v\infty}) \tag{13}$$

The gas pressure on exchanging face is equal to atmospheric pressure:

$$\left[ \langle P_g \rangle^g \right] = P_{atm} \tag{14}$$

Since the brick is placed on the swing of the dryer, the bottom face does not exchange heat with hot air. Then, we assume that the bottom face (y=0) is adiabatic and impermeable face.

$$\left[ \lambda_{eff} \frac{\partial \langle T \rangle}{\partial X_i} + \Delta H_{vap} \rho_l \langle V_l \rangle n_i \right] = 0 \tag{15}$$

$$\left[ \rho_l \langle V_l \rangle + \langle \rho_v \rangle^g \langle V_v \rangle \right] n_i = 0 \tag{16}$$

$$\left[ \frac{\partial \langle P_g \rangle^g}{\partial X_i} \right] = 0 \tag{17}$$

For heat and mass convection, the convective heat and mass transfer coefficients were listed in Table 1 [16].

**Table 1:** Convective heat and mass transfer coefficients

	Rectangular holes	Brick faces
$h_t$	$\frac{\lambda \times 0.332 \times R_e^{1/2} \times P_r^{1/3}}{L_c}$	$\frac{\lambda \times 0.023 \times R_e^{4/5} \times P_r^{1/3}}{L_c}$
$h_m$	$\frac{D_{A,B} \times 0.332 \times R_e^{1/2} \times S_c^{1/3}}{L_c}$	$\frac{D_{A,B} \times 0.023 \times R_e^{4/5} \times S_c^{1/3}}{L_c}$
Validity	$R_e < 5 \times 10^5 \quad P_r \geq 0.6 \quad S_c \geq 0.6$	
	$R_e = \frac{\rho_a w_a L_c}{\mu_a}$	$P_r = \frac{c_a \mu_a}{\lambda_a} \quad S_c = \frac{\theta_a}{D_{A,B}}$

With:

$h_t$  :the convective heat transfer coefficient( $W/m^2\text{°C}$ )

$h_m$ :the convective mass transfer coefficient( $W/m^2\text{°C}$ )

$D_{A,B}$  is the vapor diffusion in air given by:  $D_{A,B} = D_{\text{vap,air}} = 0,26 \times 10^{-4} [m^2/s]$

$L_C = 0.3 \text{ m}$  is the characteristic length of the brick.

### 3. Solution method

The equations set, with initial and boundary conditions has been solved numerically using the Control Volume Finite Element Method (CVFEM) [17-18]. The advantages of this method are (i) It ensures the flux conservation (ii) the used control volumes present more faces, that makes it possible to avoid the numerical diffusion. (iii) The control volume is composed of triangular elements that improve the grid flexibility.

#### 3.1 Mesh generation

For the mesh generation, we use the free mesh generator Gmsh [19]. The brick domain is divided first in six-node prisms. To create the polygonal control volumes around each node in the finite element grid, the centroids of the triangular elements (bases of prisms) are joined to the midpoints of the corresponding sides (Fig. 3). Then we developed a Fortran program called “Geomet Generator” allowing the reading of the Gmsh mesh file (\*.msh) and the construction of control volumes.

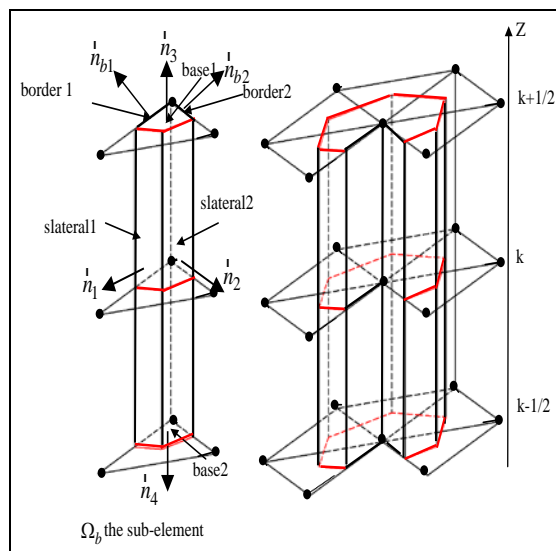


**Figure 3:** Control volume and sub-volume.

Geomet Generator generates a ‘Geomet.g’ file containing the control volumes Data structures. This file will be then used by our main program called “porous drying simulator”.

#### 4. Results and Discussions

This section is devoted to the numerical results obtained from the simulation which is applied to the drying of porous brick for two cases namely with and without vibration.

We use free mesh generator Gmsh to achieve three-dimensional meshing (Fig. 4) to numerically simulate the three-dimensional phenomenon of vibrating drying of whole brick.

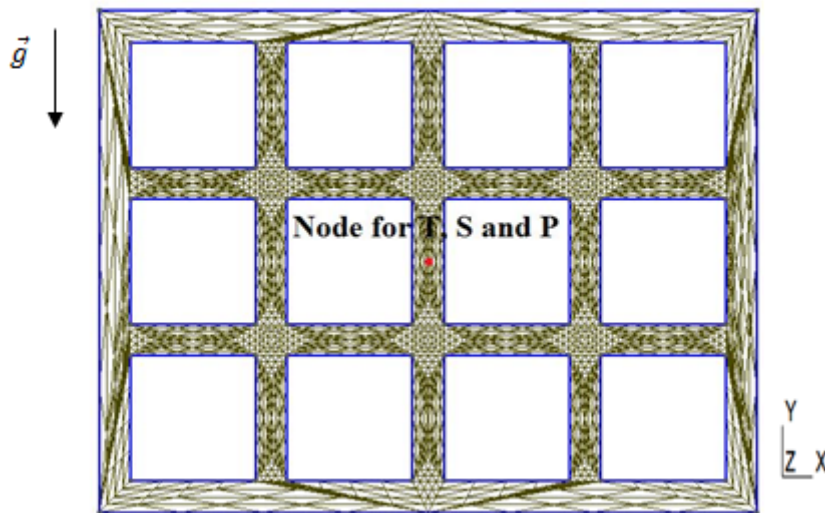


**Figure 4:** Mesh generation by Gmsh.

The operating conditions, which are listed in Table 2, are taken the same of a typical industrial drying process and we kept the same operating conditions for both cases with and without vibration.

**Table 2:** Operating conditions

$T_{amb}$	$T_{ini}$	$S_{ini}$	$C_{Vamb}$	$P_{amb}$	$P_{ini}$
(°C)	(°C)	(%)		(atm)	(atm)
<b>110</b>	<b>20</b>	<b>50</b>	<b>0.01</b>	<b>1</b>	<b>1</b>

Referring to the time evolution of temperature, liquid saturation and gas pressure for the two cases with and without vibration which are depicted in Figs. 6-9, we can clearly observe the three conventional drying phases:

- The transient heating phase

- The constant drying rate phase
- The decreasing drying rate phase:
  - First decreasing drying rate period
  - Second decreasing drying rate period

From Fig. 5, we note that the vibration accelerates the drying process. Moreover it is clearly noticed that the isenthalpic phase is slightly longer for the case of classic drying that means that the vibration highly enhances the heat and mass transfer and hence reduces the drying time.

Also referring to Fig. 6, we can observe a rapid decrease of liquid saturation for the vibration case compared to the classical drying one. Similar behavior is noticed from the gaseous pressure time evolution (Fig.7) where the most intense evaporation occurred earlier during the vibrating drying.

Since from the time evolution of liquid saturation for one node we cannot properly determine the whole drying time, we depicted in figure 8 the moisture content variation for the whole brick. From this figure it is clearly noticed that the drying period during the vibrating drying is shorter compared to the classical drying.

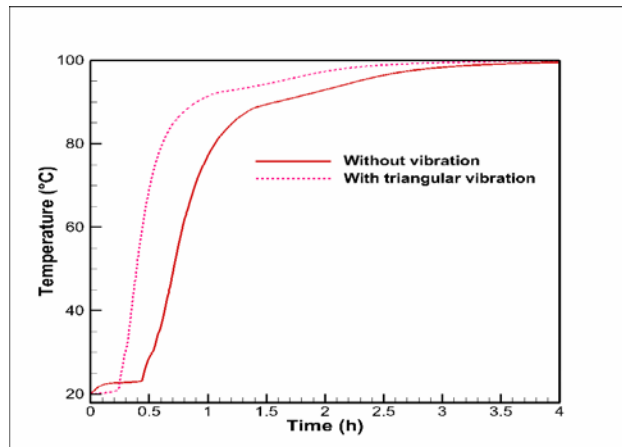


**Figure 5:** Comparison of the evolution of temperature

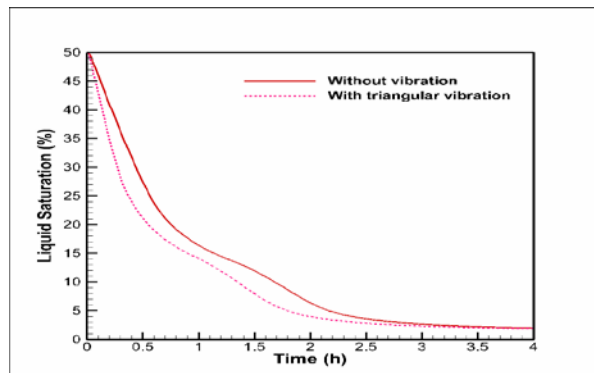


**Figure 6:** Comparison of the evolution of liquid saturation

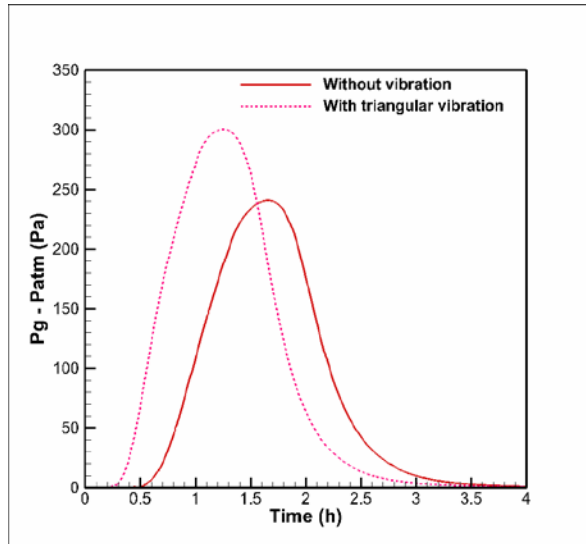


**Figure 7:** Comparison of the time evolution of gaseous pressure

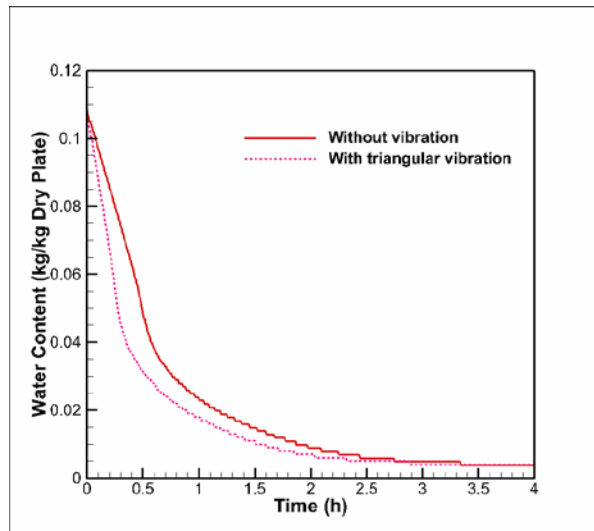


**Figure 8:** Comparison of the time evolution of water content

In order to better observe the mechanisms of 3D vibrating drying process, we showed in Fig. 9 the 3D spatiotemporal evolutions of temperature, liquid saturation and gas pressure of the whole brick after 40 min of vibrating drying. We can notice from this figure that the presence of three orthogonal exchanging faces forces the liquid saturation to be very low at the top corners and given the fact of the gravity, it is clear that only the core of whole brick and especially the bottom face retains a high value of liquid saturation. Moreover, the temperature and pressure fields allow more subtle phenomena to be observed. The temperature gradient is required to supply the energy necessary for the evaporation which occurs rapidly and intensively near the exchanging faces. Also the temperature varies significantly in space only in the region of vapor migration (gaseous Darcy's flow and vapor diffusion). The pressure gradient that exists in this region results from a cross diffusion effect of vapor and air, and in the domain of free water, almost no pressure gradient exists.

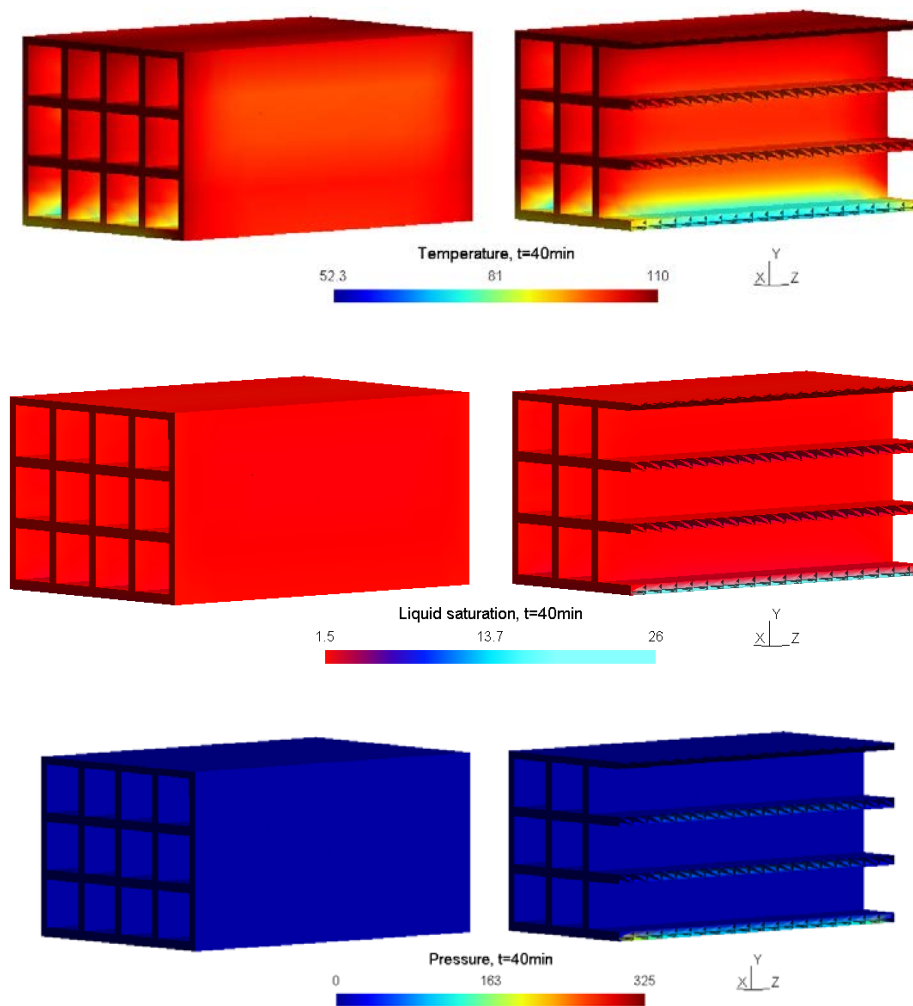


**Figure 9:** Distribution of the temperature, the liquid saturation and the gaseous pressure inside whole brick.

In order to exhibit clearly the effect of three-dimensional heat and mass transfer especially in the core of the brick, we choose the slices view to represent the distribution of temperature, liquid saturation and gaseous pressure in the three conventional phases of the drying process (Figs. 10-12):

The transient heating period: this is a very short period in the light of the overall drying time. It corresponds to the evolution of the temperature of the material to the wet bulb temperature which is

- ❖ characteristic of the drying environment accompanied by the evaporation. Though, a slight depression was observed (Fig. 10).
- ❖ The constant drying rate period: it is a time of constant rate of drying. All the heat supplied to the brick is consumed by the evaporation of water to the solid surface whose temperature is evolving to the wet bulb, homogenizes and remains constant. However, the gas depression reduces without canceling (Fig. 11).
- ❖ The decreasing drying rate period (first and second phases): it is characterized by evaporation inside

the environment and diffusion to the surface. Also in contrast, the air diffuses inwardly. Hence the occurrence of evaporation front in the brick, characterized by an increase in temperature, a significant gradient of liquid content then a decrease in the density and a gaseous overpressure.

When the front reaches the axis, the brick is in heat and moisture equilibrium with the external environment. We note also that the two bottom corners of the whole brick dry the last since they present the greatest amount of water that comes from accumulating by gravity .

After 2 h of drying (Fig.12), the process is well established. However, the exchanging faces are heated both by convective heat transfer and by the latent heat associated with the vapor that condenses at the surface. The pressure is clearly observed inside the brick whose liquid evaporation is important. As a result, it has very high values in the core of the brick and it is zero on the outer sides. Moreover, the liquid saturation decreases gradually from the center towards the exchanging face.

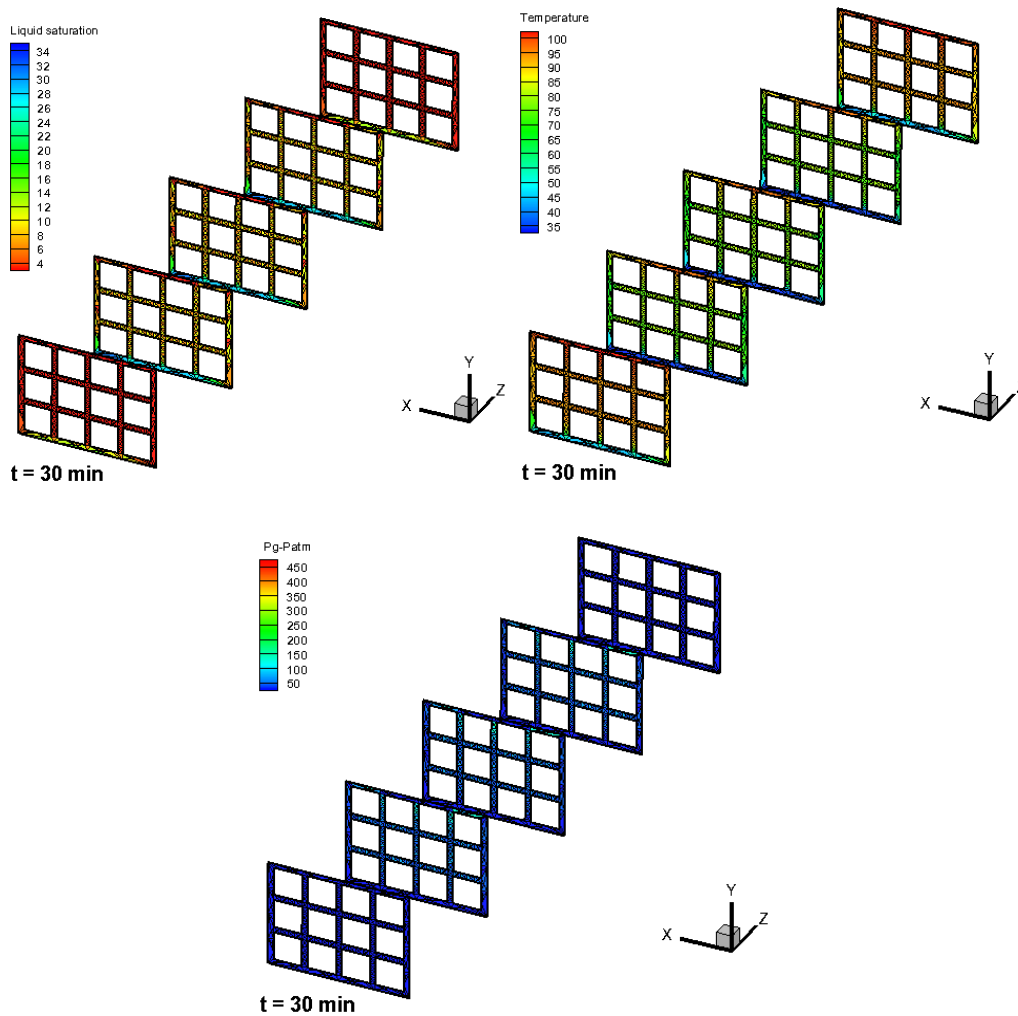


**Figure 10:** Distribution of the temperature, the liquid saturation and the gaseous pressure after 30 minutes.

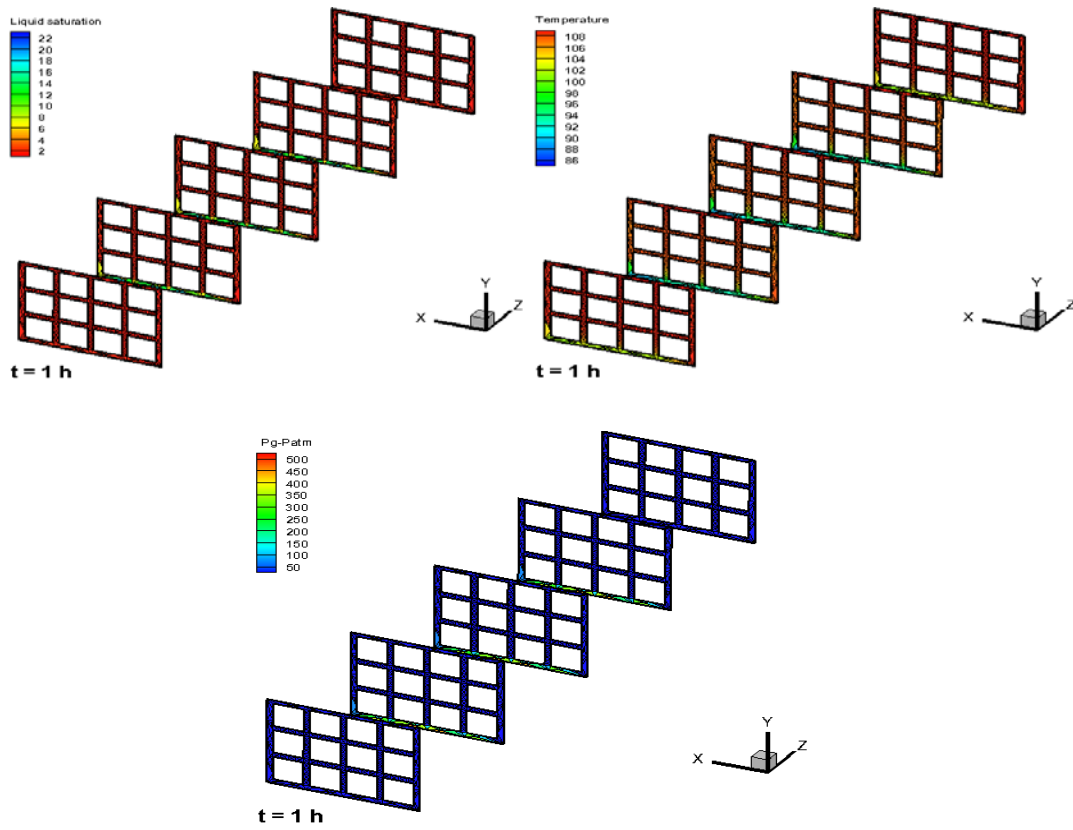


**Figure 11:** Distribution of the temperature, the liquid saturation and the gaseous pressure after 1h

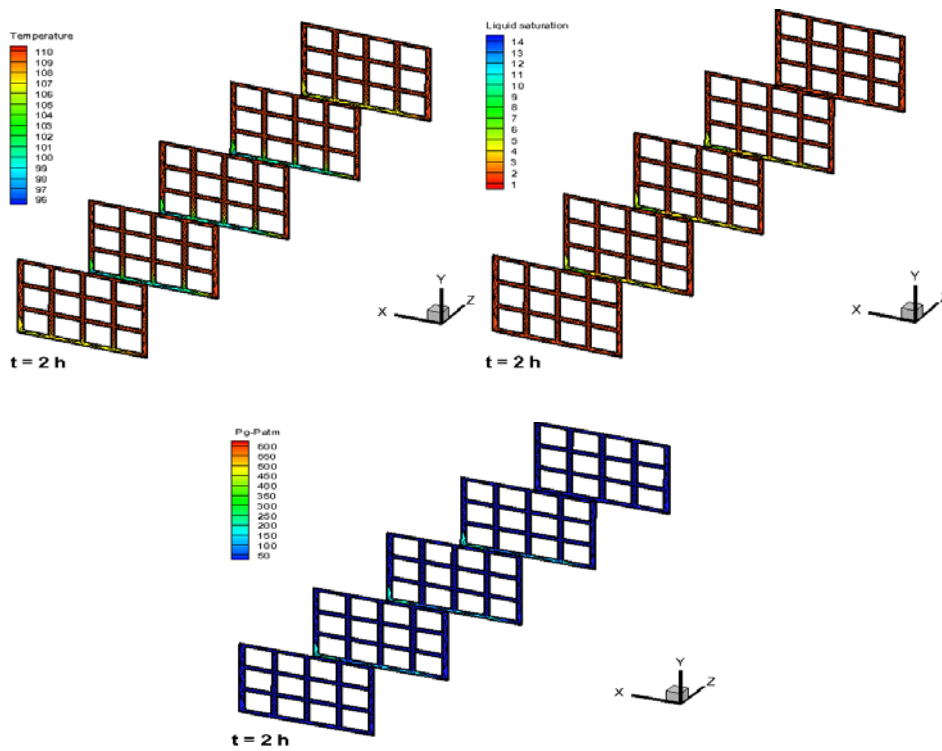


**Figure 12:** Distribution of the temperature, the liquid saturation and the gaseous pressure after 2h.

## **5. Conclusions**

In this presented study, a 3-D numerical simulation has been developed to analyze the heat and mass transfer mechanisms that arise during vibrating drying of unsaturated porous medium.

In order to quantify these effects, a comparison between two cases of convective drying was investigated namely are: with external triangular vibration and classical drying (without vibration).

Referring to the numerical results, the external vibrations highly enhance the heat and mass transfer during the drying process and the drying time is reduced by 20%.

Finally, this numerical model successfully simulates the evolution of the different phases of convective of whole brick drying.

## **References**

- [1] S.M. Beck, H. Sabarez, V. Gaukel and K. Knoerzer, “Enhancement of convective drying by application of airborne ultrasound - A response surface approach”, *Ultrasonics Sonochemistry*, Vol. 21, pp. 2144-2150, 2014.
- [2] Colin J., Chen W., Casalinho J., Ben Amara M.E.A., Ben Nasrallah S., Stambouli M. and Perré P. “Drying intensification by vibration: fundamental study of liquid water inside a pore”. The 20th International Drying Symposium (IDS 2016), Gifu, JAPAN, 7-10 August 2016.
- [3] E.A. Kolchanova and N.V. Kolchanov, “Vibration effect on the onset of thermal convection in an inhomogeneous porous layer underlying a fluid layer”, *International Journal of Heat and Mass Transfer*, Vol. 106, pp. 47-60, 2017.
- [4] G. Gershuni, D. Lyubimov, “*Thermal Vibrational Convection*, Wiley, New York, 1998.
- [5] V. Demin, G. Gershuni, I. Verkholantsev, “Mechanical quasiequilibrium and thermovibrational convective instability in an inclined fluid layer”, *Int. J. Heat Mass Transfer* 39 (9) (1996).
- [6] S. Zenkovskaya, “Effect of high-frequency vibration on filtration convection”, *J. Appl. Mech. Tech. Phys.* 33 (5) (1992) 691–695.
- [7] S. Zenkovskaya, T. Rogovenko, “Filtration convection in a high-frequency vibration field”, *J. Appl. Mech. Tech. Phys.* 40 (3) (1999) 379–385.
- [8] G. Bardan, A. Mojtabi, “On the Horton–Rogers–Lapwood convective instability with vertical vibration: Onset of convection”, *Phys. Fluids* 12 (11) (2000) 2723–2731.
- [9] Arun S. Mujumdar & Karoly Erdesz, “Applications of vibration techniques for drying and

agglomeration in food processing”, *Drying Technology* Vol. 6, Iss. 2, 1988.

- [10] Rysin, A.P., “Theory and technology of food product drying in fluidized vibration bed, *Drying of Solids*”, International Science Publisher and Oxford & IBH publishing Co. PVT. Ltd., New York, 1992; pp. 86–99.
- [11] R. Rzig, N. Ben Khedher and S. Ben Nasrallah, “A 3-D numerical heat and mass transfer model for simulating the vibration effects on drying process”, *Heat Trans Asian Res.*, Vol. 46 (2), pp. 1-18, 2017.
- [12] Ferguson, W. and Turner, I.W., (1995) “A Comparison of the Finite Element and Control Volume Solution Techniques Applied to Timber Drying Problems Below the Boiling Point”, *Int. J. Num. Meth. Eng.*, 38 (9), pp. 451-467.
- [13] Ferguson, W. and Turner, I.W., (1995) “A Study of Two-Dimensional Cell-Centered and Vertex-Centered Control-Volume Schemes Applied to High Temperature Timber Drying”, *J. Num. Heat Transfer, Part B: Fundamentals*, Vol. 27, pp. 393-415.
- [14] Turner, I.W. and Ferguson, W.J., (1995) “An Unstructured Mesh Cell-Centered Control Volume Method for Simulating Heat and Mass Transfer in Porous Media: Application to Softwood Drying, Part I: The Isotropic Model, *Appl. Math. Modeling*”, Vol. 19.
- [15] Turner, I.W. and Ferguson, W.J., (1995) “An Unstructured Mesh Cell-Centered Control Volume Method for Simulating Heat and Mass Transfer in Porous Media: Application to Softwood Drying, Part II: The Anisotropic Model, *Appl. Math. Modelling*”, Vol. 19.
- [16] F.P. Incropera and D.P. De Witt, “*Fundamentals of Heat and Mass Transfer*”, John Wiley & Sons, New York, USA, 2002.
- [17] Balliga B.R. and Patankar S.V., “A new finite-element formulation for convection–diffusion problems”, *Numer Heat Transfer* 1980, 3, 393–409.
- [18] Balliga B.R. and Patankar S.V., “A control-volume finite element method for two-dimensional fluid flow and heat transfer”, *Numerical Heat Transfer* 1983, 6, 245–6.
- [19] Christophe Geuzaine and Jean-François Remacle, “Gmsh: A 3-D finite element mesh generator with built-in pre- and post-processing facilities”, *International Journal for Numerical Methods in Engineering* 2009, 79 (11), pages 1309–1331, 10.